

Mechanical Characterization and Finite Strain Constitutive Modeling of Electrospun Polycaprolactone under Cyclic Loading

Rebecca B. Dupaix^{*}, Jennifer E. Davidson Hosmer^{**}

Department of Mechanical Engineering, The Ohio State University, Columbus, OH 43221, USA

Abstract

Electrospun polymers have potential for use as tissue engineered scaffolds, yet in this environment they must be able to withstand multiple cycles of loading, slightly elevated temperatures, moisture, and other degrading chemical interactions. In this work, the effects of cyclic loading, temperature, and moisture on electrospun polycaprolactone are investigated through tensile testing of dogbone-shaped specimens. Effects of fiber alignment on the macroscopic mechanical behavior are investigated by comparing samples collected on a flat plate with samples collected on a rotating cylinder. Small temperature changes had only a small effect, but moisture significantly degraded the performance of the material. In cyclic testing, the mechanical behavior changed significantly after the first cycle, suggesting that damage to the original structure occurs when first loaded. A hyperelastic representative volume element-based constitutive model was modified to capture the effect of cyclic damage and was found to reproduce the general trend quite well.

Keywords: Electrospinning; Mechanical Behavior; Polycaprolactone; Cyclic Loading; Constitutive Model

1. Introduction

Electrospun polymeric materials have potential use in a wide variety of applications, including as a promising scaffold for tissue engineering (see, for example two recent reviews by Martins et al. (2008) and Sill and von Recum (2008)). Through the electrospinning process, a nonwoven fabric consisting of nano-scale fibers is created. The nano-scale structure of the fibers combined with the connected porous structure between the fibers creates a surface that is highly amenable to cell seeding and proliferation. This work seeks to better characterize the mechanical behavior of electrospun polycaprolactone (PCL) under cyclic loading and to explore the influence of other relevant environmental variables. An understanding of the behavior of the material is particularly important in bio-scaffolding, where the behavior under cyclic loading and the influences of temperature and moisture are critical.

Electrospinning is a popular fabrication method due to its ability to create nanoscale structures with a high surface area to mass ratio and very high porosity when spun into three-dimensional scaffolds. In addition, it is a fairly simple, inexpensive processing technique that can be used to optimize the size, shape, and orientation of the electrospun fibers. These attributes allow electrospun nonwoven mats to be used in many applications, such as molecular filtration membranes, electrical/optical equipment, biosensors, catalytic nanofibers, reinforcing fibers in composite materials, and more recently in drug delivery and wound dressings (Pham et al. 2006; Li et al. 2005; and Luong-Van et al. 2006).

The mechanical properties of the electrospun mat strongly depend on the processing conditions. These include the properties of the solution, processing parameters, and ambient conditions (Pham et al. 2006 and Inai, Kotaki, et al. 2005). The variable that most influences the fiber size and the morphology is the solution viscosity. Increasing the polymer concentration also causes the fiber diameter to increase (Pham et al. 2006). The type of collector directly affects the morphology of the fabric. Metal plate collectors produce smooth fibers in a nonwoven randomly oriented matrix. Rotating cylindrical collectors can produce matrices with aligned nanofibers (Pham et al. 2006).

In this work, we investigate the mechanical behavior of electrospun material with fibers that have been produced by two different spinning methods and collected on two different surfaces, one a flat plate and the other a rotating cylinder. A constitutive model is then proposed to explain some of the results from the cyclic loading experiments.

Prior research on the mechanical behavior of electrospun materials has focused on modulus, tensile strength, and elongation to failure, often investigating the effects of changing processing conditions or morphology on these properties (Lee et al. 2003; Lee et al. 2007, and Cha et al. 2006). A recent paper by Johnson et al. (2009) looked at the change in properties of electrospun poly(caprolactone) that has been exposed to in vitro conditions, and saw a drop in

^{*}Email: dupaix.1@osu.edu

^{**}Current address: 3825 Cunningham Ct., Fairfield, OH 45011, USA

modulus, strength, and elongation to failure. Relatively little data has been published on the behavior under cyclic loads, in spite of the clear relevance for tissue engineering applications (Duling et al. 2008). More recent papers have investigated the properties of individual fibers (Lim et al. 2008 and Wong et al. 2008).

Little prior modeling work has been done on electrospun polymers. Engelmayr and Sacks (2006) have developed one model that predicts the role of the extracellular matrix (ECM) formation on the effective stiffness of a nonwoven tissue-engineered scaffold in bending. This paper utilized a structural model to predict the effective stiffness of a needled nonwoven tissue-engineered scaffold. The findings from this study showed that needled nonwoven scaffolds are not always isotropic, that crimped polyglycolic acid (PGA) and poly-L-lactic acid (PLLA) fibers act more like springs than straight rods, and that the main function of collagen reinforcement in nonwoven tissue-engineered scaffolds is an increase in the number of rigidly bonded cross-over points between fibers (Engelmayr and Sacks 2006). Work by Courtney et al. (2006) used the structural-based model to model the difference in mechanical behavior depending on the mandrel speed during fabrication. In this work, we use a simpler RVE-based model to illustrate the effect of cyclic loading, but the ideas of evolving damage and morphology could be extended to the structural-based modeling ideas from the Sacks group.

2. Materials and Methods

Table 1 shows the parameters used to produce the electrospun poly(caprolactone) (PCL) samples. The PCL used had a Molecular Weight of 65,000 (Sigma-Aldrich, St. Louis, MO), a melting temperature of $\sim 60^{\circ}\text{C}$, and a glass-transition temperature of $\sim 65 - 60^{\circ}\text{C}$.

Table 1. Parameters Used to Produce Electrospun PCL Samples.

Solution type	PCL in Acetone
PCL weight percentage	12 wt. % for Indirect Spinning 25 wt. % for Direct & Horizontal Spinning
Capillary flow rate	20 ml/hr
Electric field	24 kV
Spin time	10 – 15 minutes
Distance from tip to collector	15 cm (direct) & 18 cm (indirect)

Two types of electrospinning were used in this work: direct and indirect. Most of the PCL samples that were used in this study were directly spun. For the directly spun samples, a 25 wt. % solution was used. For the indirectly spun samples, a 12 wt. % solution was used. For indirect spinning, the solution passed from the syringe through a plastic lead to a distant point where the tip was attached. The distance from the tip to the collector was 18 cm. For direct spinning, the tip was directly attached to the syringe and the tip was 15 cm from the collector.

Horizontal electrospinning was conducted using the direct electrospinning method, but instead of collecting the material on a flat steel plate, the PCL was spun horizontally onto a $\frac{1}{2}$ inch diameter mandrel, that was rotated at 2500 rpm. After the electrospinning process was complete, the cylindrical sample was cut longitudinally to produce a 3 inch by 1.5 inch sheet that was then ready to be cut into dogbone samples that were either longitudinally aligned (along the length of the mandrel) or circumferentially aligned (around the circumference of the mandrel).

Samples were cut in the shape of a dogbone using a metal template, No. 15 stainless steel surgical blades, and a 6 mm biopsy punch. The gauge length was 20.0 mm, the width 2.4 mm, and the thickness ranged from about 0.2 mm to 0.5 mm, depending on the spin time of the samples.

Tensile tests were conducted on an Instron model 5869 electromechanical extended range test frame running Bluehill2 software, with a 500 N load cell and pneumatic grips to hold the samples. For the tests that were run at or slightly above 37°C , an Instron model 3119-409 temperature chamber was utilized. For the soak tests, samples were placed in a 37°C bath of distilled water for the prescribed length of time and were removed from the bath just prior to testing at room temperature.

Cyclic tensile tests were conducted at an extension rate of 0.8 mm/s. The main testing program considered in this work is as follows. The sample is pulled to 10% strain, returned to zero, pulled to 20% strain, returned to zero, and finally pulled to failure. A limited number of other tests probed the effects of multiple cycles, different strain levels, or allowing time between cycles.

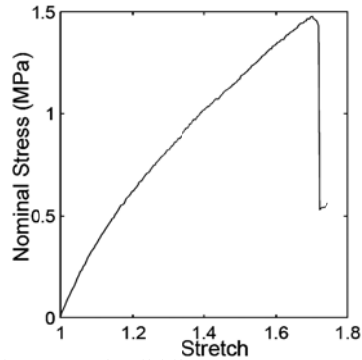


Figure 1. Load until failure test – stress vs. stretch.

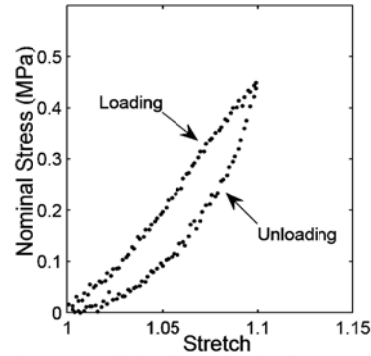


Figure 2. Cyclic loading and unloading - stress vs. stretch with 10% strain.

3. Test Results

3.1 Cyclic Test Results

Previous work by Duling, et al. (2008) found that during load-to-failure testing of electrospun PCL the material exhibited a concave-down shape (see Figure 1), somewhat counter-intuitive since a rubbery material would typically strain harden, especially at large strains. In that work, they also conducted a limited number of cyclic experiments, and observed in these a significant change in behavior upon subsequent loading. Based on this result, we begin with a more extensive treatment of cyclic tests, in order to elucidate the change in behavior upon repeated loadings.

We suggest that the reason for the concave down shape is that the electrospun PCL material starts out relatively stiff, but softens upon deformation due to accumulating damage, such as branching points failing. The cyclic results, described below, support this conclusion, which is then used as motivation for the proposed model.

Figure 2 displays the stress-strain behavior of an electrospun PCL sample loaded to a strain of 10% and unloaded back to zero. The shape of the stress-strain curve clearly changes upon unloading; the unloading portion follows a concave up trend, more commonly seen in polymeric and rubber materials.

Figure 3(a) shows test results for two indirectly spun samples and Figure 3(b) shows results for two directly spun samples, both cycled once to 10% strain, once to 20% strain, and finally loaded to failure. In both cases, the stress-strain curves follow a different shape upon unloading and reloading to the same strain level, but upon continued straining, the curves return to the softening/damage-induced concave-down shape.

The electrospun PCL samples prepared by direct spinning had higher failure stresses and higher elongation at failure than the samples produced by indirect spinning. It is important to note that these samples were produced with different PCL concentrations. The indirectly spun samples were 12 wt. % PCL and the directly spun samples were 25 wt. % PCL. It is unclear whether the extreme difference between the indirectly spun samples and the directly spun samples was caused more by the direct spinning or the increase in the weight percentage, but it was likely a combination of the two.

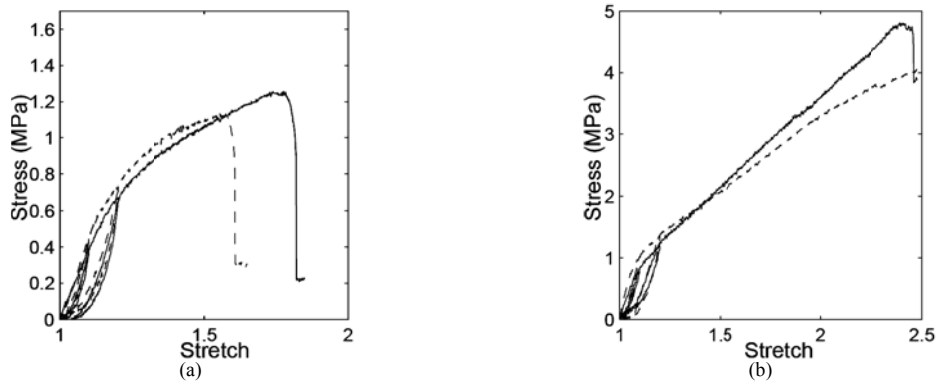


Figure 3. Cyclic test: stretch vs. stress. (a) indirect spinning, (b) direct spinning

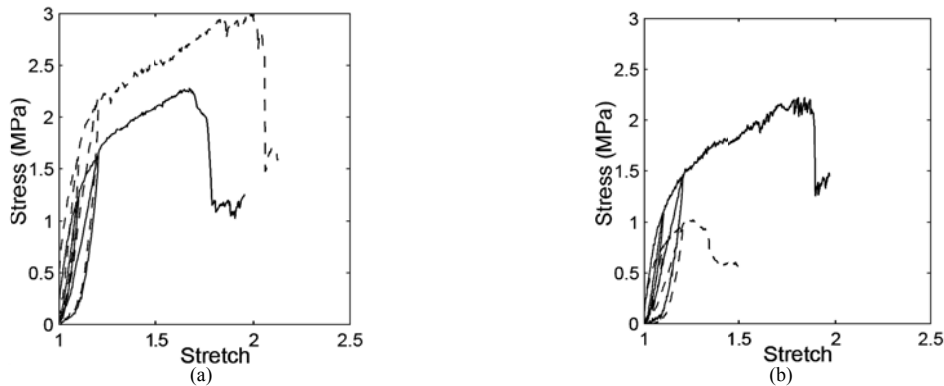


Figure 4. Cyclic test (a) Longitudinally aligned; (b) Circumferentially aligned.

Results demonstrate that the material is more durable when it is directly spun. The failure stress of the directly spun samples in Figure 3(b) was more than twice as high as those in Figure 3(a). The elongations of these samples were also higher. Although the failure properties are very different, the shape of the stress-strain curves and the general trends were identical.

3.2 Fiber Alignment Test Results

Figure 4 shows results for samples that were longitudinally and circumferentially aligned and directly spun. The longitudinally aligned samples tended to give more repeatable results than the circumferentially aligned samples. On average, the longitudinally aligned and circumferentially aligned material displayed similar trends. The failure stress and total elongation were alike and even the curve leading up to the breaking point was similar. Comparing these samples to the isotropic directly spun samples in Figure 3(b), the aligned samples were weaker in terms of failure stress and maximum elongation. The expectation prior to running tests on these samples was that the circumferentially aligned samples would exhibit more strength because their fibers should be more aligned. The results did not show this. If anything, the circumferentially aligned samples were the weakest of the three types of samples. This may have been caused by the slow mandrel speed. The maximum drill speed of 2500 rpm may not have been fast enough to produce effective alignment.

Figure 5 shows the results of a set of experiments designed to probe the effects of conducting multiple cycles at each strain level. In this case, 5 cycles were completed at 10% strain, followed by 5 cycles at 20% strain, and finally the sample was pulled to failure. The three samples shown in Figure 5 were indirectly spun. The resulting shape of the stress-strain curves is very similar to the results shown in Figure 3(a), with the exception that the failure stresses are slightly lower than in the experiments with only one cycle at each strain level. Multiple cycles likely weakened the material. The overall strain to failure, however, was essentially unchanged between the two sets of tests.

Figure 6 shows the results from experiments designed to probe the effects of cycling at higher strain levels. For these tests, the samples were strained to 30% and 50% with one cycle at each strain level, followed by strain to

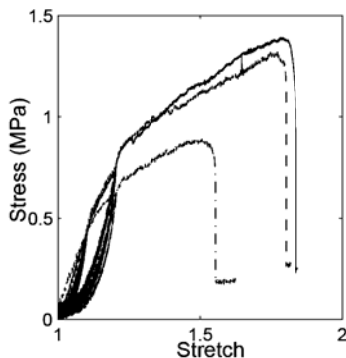


Figure 5. Indirect spinning, 5 cycles at 10% and 20% strain stress vs. stretch.

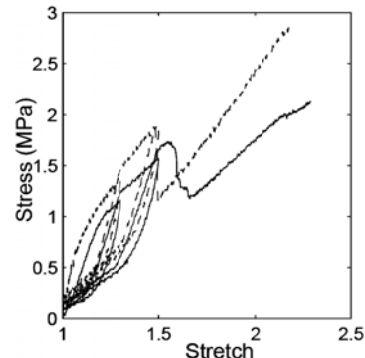


Figure 6. Indirect spinning, cycles at 30% and 50% strain stress vs. stretch.

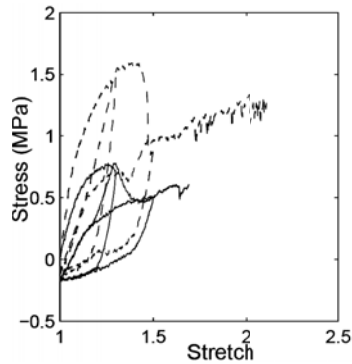


Figure 7. Circumferentially aligned stress vs. stretch, cycles at 30% and 50% strain.

failure. The cyclic portion of these two samples showed the same general trends as cyclic tests to lower strain levels. In some samples, a drop in stress was observed shortly after the last cycle that may indicate some partial failure of the sample.

This testing protocol was also run on longitudinally aligned and circumferentially aligned samples with an example of two circumferentially aligned samples shown in Figure 7. The stress-stretch curve shows similar behavior to the previous samples but exhibits more catastrophic damage. This increased damage is most apparent in the second cycle of the test where the material is being strained to 50%. The results here indicate that the specimen becomes softer with cycling at larger strains. The longitudinally aligned samples displayed a similar trend.

3.3 Cyclic Test Results with Hold Periods

To probe the effects of time and possibly damage recovery during the experiments, cyclic tests were conducted where the material was given time to rest between groups of cycles. The first of these tests involved 5 cycles each at 10%, 20% and 30% strain levels. In between each group, the sample rested for 60 seconds at zero strain. At the end, the sample was stretched to failure.

Figure 8(a) shows very similar stress-stretch behavior to the rest of the cyclic tests, indicating that holding at zero strain has little effect on the material behavior. In Figure 8(b), the sample was subjected to a load history of 3 cycles each at 10, 20, and 30% strain, with 600 seconds of 0-strain hold in between each group of cycles. Again, the similarity in the stress-stretch trends indicates little influence of this hold time on the material behavior.

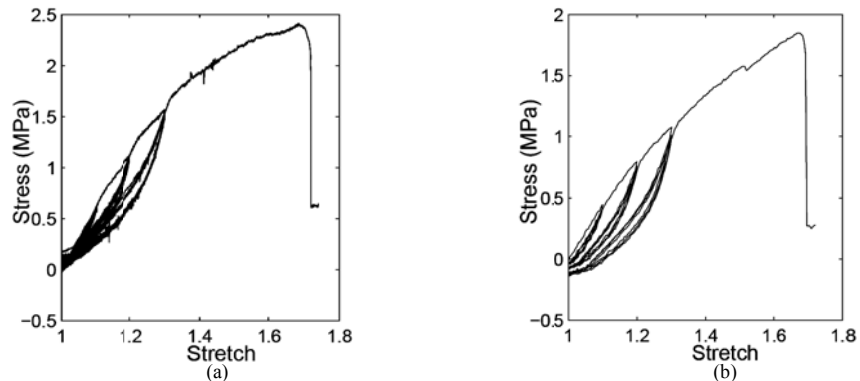


Figure 8. Cyclic test with (a) 60 sec and (b) 600 sec intermediate holds: stress vs. stretch.

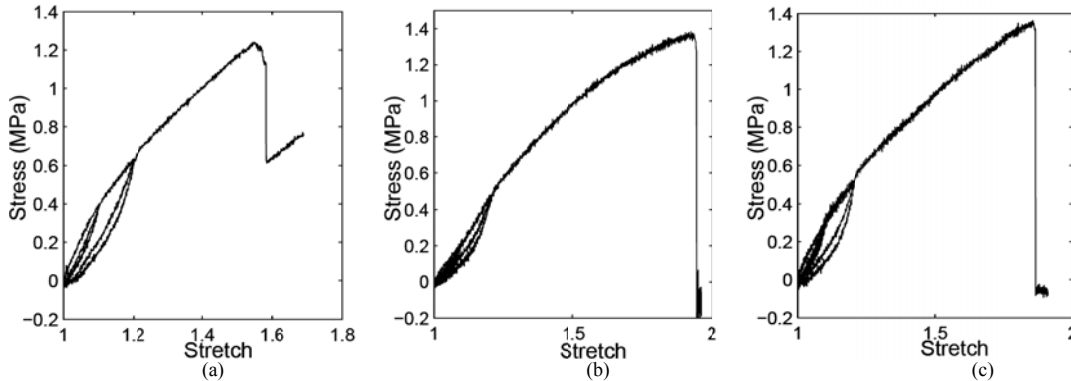


Figure 9. Stress vs. stretch: cyclic test at (a) 37°C, (b) 40°C, and (c) 45°C.

3.4 Temperature Test Results

A few samples were tested using the initial cyclic testing procedure (single cycles to 10 and 20% strain) using the Instron temperature chamber set to 37 °C, 40°C, and 45 °C. All samples were produced via indirect electrospinning. The results, shown in Figure 9, showed only small differences between the results at room temperature and the results at 37, 40, and 45 °C. The failure stress and elongation at failure were slightly higher at these temperatures than was observed in the indirectly spun samples tested at room temperature. The main difference was that the hysteresis between loading and unloading decreased in magnitude as the temperature increased. This can be seen when comparing Figure 9 to the samples at room temperature (Figure 3(a)). One possible reason for the smaller difference in cyclic loading is that as the temperature increases, the microstructure of the fibers or of the nonwoven mat may begin to change. This change in microstructure could cause some of the weaker branching points to strengthen, reducing the amount of cyclic damage and somewhat strengthening the material.

3.5 Soak Test Results

The influence that moisture could have on the electrospun PCL samples was studied by soaking the samples in a distilled water bath prior to testing them. The time periods for the soak tests were three, six, and nine weeks. All of the samples for this series of tests were produced using direct electrospinning and the tests used the main cyclic loading history of one cycle at 10% strain, a second cycle at 20% strain, followed by load to failure.

Figure 10(a) shows the results for samples that were collected on a flat plate and soaked for 3 weeks. Compared with material that was not soaked (Figure 3(b)), the pattern of the cyclic portion is very similar. However, after three weeks of soaking, the samples are seen to fail at a much lower stress level (1-1.5 MPa as compared with 4-5 MPa without soaking) and a correspondingly much lower failure strain. This indicates that exposure to water significantly weakens the samples.

Figure 10(b) shows the results of flat plate collected samples tested after 6 weeks of soaking. The failure stress and elongation at failure were similar to those seen in the three week soak tests.

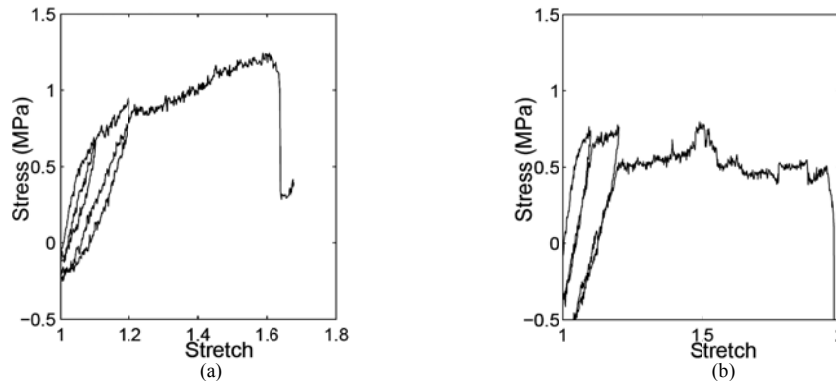


Figure 10. Soak test, flat plate collector, (a) 3 weeks, (b) 6 weeks.

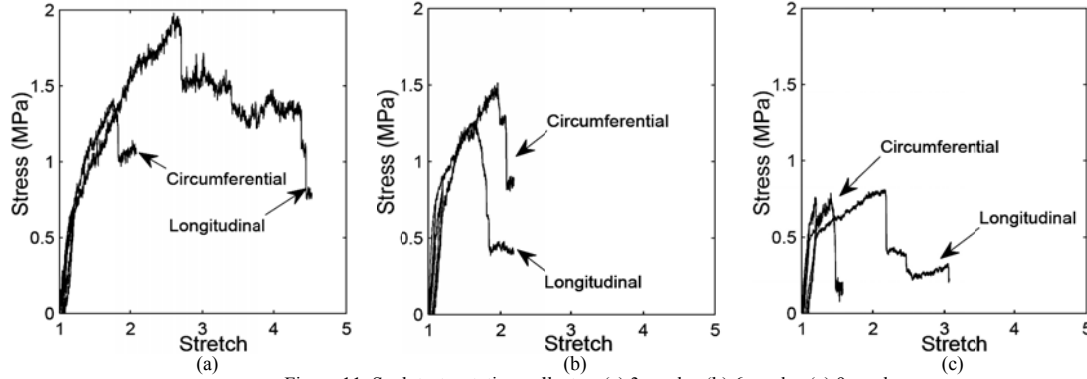


Figure 11. Soak test, rotating collector, (a) 3 weeks, (b) 6 weeks, (c) 9 weeks

Figure 11 shows the results of three, six, and nine week soak tests for longitudinally and circumferentially aligned samples. From these figures it is clear that as the soak time increases, the failure stress levels decrease and the maximum elongation decreases. This again indicates that water weakens the electrospun PCL over time. As a general trend, the circumferentially aligned samples were weaker than the longitudinally aligned samples, though this is masked in the 6 week soak test (Figure 11(b)) because of a longitudinal sample that failed rather early.

The trend of fiber damage and fiber elongation in the PCL samples during the cyclic loading seems to remain throughout the soak tests. The results demonstrate that water is causing a significant weakening as exposure time increases.

4. The Constitutive Model

Many polymers and biomaterials exhibit similar stress-strain behavior to rubbers. In addition, rubber models have been adapted to capture damage effects, such as the Mullins effect, with similar impact on the stress strain behavior as seen in this work (Qi and Boyce 2004). For that reason, we begin modeling electrospun PCL using the 8-chain rubber elasticity model developed by Arruda and Boyce (1993).

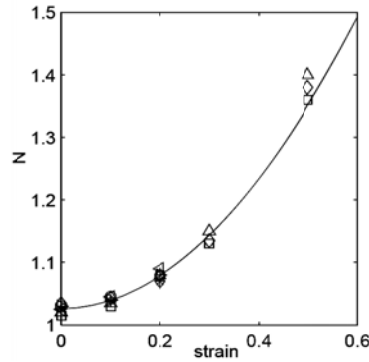
The eight chain model is able to capture the behavior of rubbers under various kinds of loading, while using only two material parameters, the limiting chain extensibility, N , and the chain (or fiber) density, n . The eight chain model includes assumptions of incompressibility, isotropy, and hyperelasticity. These assumptions do not perfectly represent the electrospun PCL because (1) the electrospun PCL is at least somewhat anisotropic, (2) although PCL in solid form is essentially incompressible, it is doubtful that electrospun PCL is incompressible because of its high porosity, and (3) we know from previous work (Duling et al. 2008) that the material exhibits some time dependence. But, for simplicity, we start here. The details of the model development can be found in Arruda and Boyce (1993), with the resulting stress-stretch relation given by

$$\sigma_1 - \sigma_2 = \frac{nk\Theta}{3} \sqrt{N} L^{-1} \left[\frac{\lambda_{chain}}{\sqrt{N}} \right] \left(\frac{\lambda_1^2 - \lambda_2^2}{\lambda_{chain}} \right), \quad (1)$$

where σ_i is the stress in the i -th direction, λ_i is the stretch in the i -th direction, $\lambda_{chain} = \frac{1}{\sqrt{3}} (\lambda_1^2 + \lambda_2^2 + \lambda_3^2)^{1/2}$, n is the chain density, k is Boltzman's constant, Θ is temperature, and L^{-1} is the inverse Langevin function, given by $L(\beta) = \coth\beta - 1/\beta$.

To model the accumulated damage, we prescribe the material constants to evolve with deformation. Structurally, this can be interpreted as follows. In the original 8-chain model, the constants N and n were related to physical crosslinks and crosslink density. Here, crosslinks might be replaced by fiber branching points. Due to damage, as these branching points are fractured, both the number of branching points and their density will have to evolve in concert, so as to satisfy conservation of mass:

$$N*n = \text{constant} \quad (2)$$

Figure 12. Relationship between N and strain.

We wish N to evolve as branching points break with accumulated strain. A phenomenological expression was developed based on curve fits to the cyclic loading and unloading data. Each curve fit determined the appropriate value of N at each level of strain, as shown in Figure 12. A second-order curve fit provides the evolution equation for N :

$$N = 1.2875\varepsilon_{\max}^2 + .0062\varepsilon_{\max} + 1.0260, \quad (3)$$

where ε_{\max} stands for the maximum strain level the material has been subjected to. The value of n at each strain is determined using the initial fit for n from the initial loading curve and subsequent values are determined using the conservation of mass requirement.

The eight chain model is used to predict the behavior under cyclic loading as shown in Figure 13. The constitutive model does a very good job of capturing the initial loading and unloading at small strains (shown here at 10% and 20%). Deviation occurs at larger strains, which suggests that something else needs to be incorporated into the model to produce a better fit for higher strains. For example, this model does not include any time dependence, though the material is known to be somewhat time dependent. It is anticipated that including time dependence in the model may improve predictions at larger strain levels. Additionally, the phenomenological fit of N versus strain could be improved with a model that accounts for a distribution of branching point strengths. Future work will also investigate incorporating anisotropy (as in Kuhl, et al. 2005) to predict the behavior of horizontally spun samples.

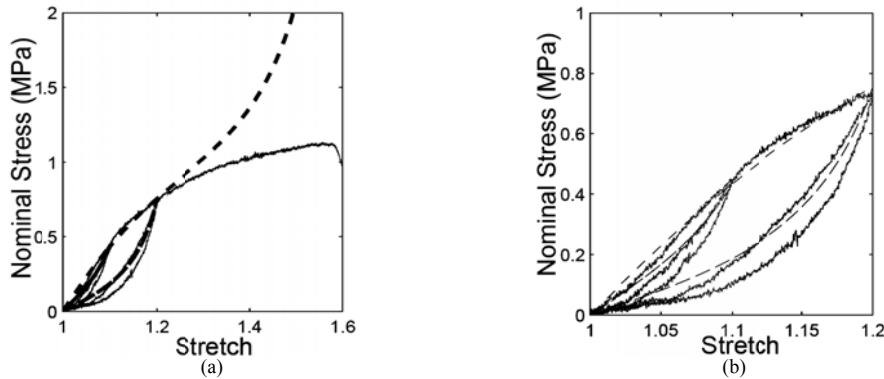


Figure 13. Experimental data vs. eight chain model prediction. The dashed curve is the model prediction.

5. Conclusion/Future Work

The goal of this research was to characterize electrospun PCL and to find an appropriate model to describe the behavior of the material under cyclic loading. Cyclic testing revealed that the material exhibits a different shape to the stress-strain curve upon unloading/reloading. This trend persists in directly and indirectly spun samples, with multiple cycles at the same strain level, and with hold periods between the cycles. The hysteresis decreases somewhat at elevated temperatures. Results also showed that exposure to moisture significantly degrades the material properties. Results comparing the behavior of longitudinally and circumferentially aligned samples with samples collected on a flat plate showed substantial differences. The samples collected on the rotating mandrel were significantly weaker.

The outcome of the constitutive modeling suggests that the modified eight chain model was able to capture the behavior of the polymeric sample at low strains, but deviation from the experimental results occurred at higher strains, possibly because of the need to include time-dependence in the model.

Another area for future study is orientation development. Preliminary results suggest that there is some underlying remodeling taking place. The polymer fibers start out very random and unaligned. As loading occurs, the fibers gradually begin to orient and become significantly more aligned by the time failure occurs. This process of remodeling shows a lot of promise considering remodeling occurs in most biomaterials. Future work should be aimed at investigating whether or not this orientation is permanent or if the sample would be able to recover. Other future modeling work could utilize an orthotropic model to capture anisotropy. If a correlation can be found between fiber alignment, anisotropy, and mechanical strength, this could be used in design to tailor mechanical properties to meet design requirements.

References

- Arruda, E.M., and Boyce, M.C., 1993 A Three-Dimensional Constitutive Model for the Large Stretch Behavior of Rubber Elastic Materials, *Journal of the Mechanics and Physics of Solids*, **41**, 389-412.
- Cha, D.I., Kim, K.W., Chu, G.H., Kim, H.Y., Lee, K.H., and Bhattarai, N. 2006 Mechanical behaviors and characterization of electrospun polysulfone/polyurethane blend nonwovens, *Macromolecular Research*, **14**, 331-337.
- Courtney, T., Sacks, M.S., Stankus, J., Guan, J., and Wagner, W.R., 2006 Design and analysis of tissue engineering scaffolds that mimic soft tissue mechanical anisotropy. *Biomaterials*. **27**, 3631-3638.
- Duling, R.R., Dupaix, R.B., Katsube, N., and Lannutti, J., 2008 Mechanical characterization of electrospun polycaprolactone (PCL): A potential scaffold for tissue engineering. *Journal of Biomechanical Engineering—Transactions of the ASME*. **130**,(1), Article Number:011006 (DOI: 10.1115/1.2838033)
- Engelmayr, G.C., and Sacks, M.S., 2006 A structural model for the flexural mechanics of nonwoven tissue engineering scaffolds. *Journal of Biomechanical Engineering-Transactions of the ASME*. **128**, 610-622.
- Inai, R., Kotaki, M., and Ramakrishna, S., 2005 Deformation behavior of electrospun poly(L-lactide-co-epsilon-caprolactone) nonwoven membranes under uniaxial tensile loading, *Journal of Polymer Science Part B-Polymer Physics*, **43**, 3205-3212.
- Johnson, J., Niehaus, A., Nichols, S., Lee, D., Koepsel, J., Anderson, D., and Lannutti, J., 2009 Electrospun PCL in vitro: a microstructural basis for mechanical property change. *Journal of Biomaterials Science-Polymer Edition*, **20**, 467-481.
- Kuhl, E., Garikipati, K., Arruda, E.M., and Gosh, K., 2005 Remodeling of biological tissue: Mechanically induced reorientation of a transversely isotropic chain network, *Journal of the Mechanics and Physics of Solids*, **53**, 1552-1573.
- Lee, K.H., Kim, H.Y., Khil, M.S., Ra, Y.M., and Lee, D.R., 2003 Characterization of nano-structured poly(epsilon-caprolactone) nonwoven mats via electrospinning, *Polymer*, **44**, 1287-1294.
- Lee, S.J., Yoo, J.J., Lim, G.J., Atala, A., and Stitzel, J., 2007 In vitro evaluation of electrospun nanofiber scaffolds for vascular graft application, *Journal of Biomedical Materials Research Part A*. (DOI: 10.1002/jbm.a.31287.)
- Li, M., Mondrinos, M.J., Gandhi, M.R., Ko, F.K., Weiss, A.S., and Lelkes, P.I., 2005 Electrospun protein fibers as matrices for tissue engineering. *Biomaterials*. **26**, 5999-6008.
- Lim, C.T., Tan, E.P.S., and Ng, S.Y., 2008 Effects of crystalline morphology on the tensile properties of electrospun polymer nanofibers, *Applied Physics Letters*, **92**(14), Article Number:141908.(DOI:10.1063/1.2857478)
- Luong-Van, E., Grondahl, L., Chua, K.N., Leong, K.W., Nurcombe, V., and Cool, S.M., 2006 Controlled release of heparin from poly(epsilon-caprolactone) electrospun fibers, *Biomaterials*, **27**, 2042-2050.
- Martins, A., Reis, R.L., and Neves, N.M., 2008 Electrospinning: processing technique for tissue engineering scaffolding, *International Materials Reviews*. **53**, 257-274.
- Pham, Q.P., Sharma, U., and Mikos, A.G., 2006 Electrospinning of polymeric nanofibers for tissue engineering applications: A review, *Tissue Engineering*, **12**, 1197-1211.
- Qi, H.J., and Boyce, M.C., 2004 Constitutive model for stretch-induced softening of the stress-stretch behavior of elastomeric materials. *Journal of the Mechanics and Physics of Solids*, **52**, 2187-2205.
- Sill, T.J., and von Recum, H.A., 2008 Electrospinning: Applications in drug delivery and tissue engineering, *Biomaterials*, **29**, 1989-2006.
- Wong, S.-C., Baji, A., and Leng, S., 2008 Effect of fiber diameter on tensile properties of electrospun poly(epsilon-caprolactone). *Polymer*. **49**, 4713-4722.